Reactions of Azine Anions with Nitrogen and Oxygen Atoms: Implications for Titan's Upper Atmosphere and Interstellar Chemistry

Zhe-Chen Wang,[*,†] Callie A. Cole,[†] Nicholas J. Demarais,[†,#] Theodore P. Snow,[‡,§] and Veronica M. Bierbaum[*,†,§]

[†]Department of Chemistry and Biochemistry, University of Colorado, Boulder, Colorado 80309, United States
[‡]Department of Astrophysical and Planetary Sciences, University of Colorado, Boulder, Colorado 80309, United States
[§]Center for Astrophysics and Space Astronomy, University of Colorado, Boulder, Colorado 80309, United States

Ⓢ *Supporting Information*

ABSTRACT: Azines are important in many extraterrestrial environments, from the atmosphere of Titan to the interstellar medium. They have been implicated as possible carriers of the diffuse interstellar bands in astronomy, indicating their persistence in interstellar space. Most importantly, they constitute the basic building blocks of DNA and RNA, so their chemical reactivity in these environments has significant astrobiological implications. In addition, N and O atoms are widely observed in the ISM and in the ionospheres of planets and moons. However, the chemical reactions of molecular anions with abundant interstellar and atmospheric atomic species are largely unexplored. In this paper, gas-phase reactions of deprotonated anions of benzene, pyridine, pyridazine, pyrimidine, pyrazine, and s-triazine with N and O atoms are studied both experimentally and computationally. In all cases, the major reaction channel is associative electron detachment; these reactions are particularly important since they control the balance between negative ions and free electron densities. The reactions of the azine anions with N atoms exhibit larger rate constants than reactions of corresponding chain anions. The reactions of azine anions with O atoms are even more rapid, with complex product patterns for different reactants. The mechanisms are studied theoretically by employing density functional theory; spin conversion is found to be important in determining some product distributions. The rich gas-phase chemistry observed in this work provides a better understanding of ion-atom reactions and their contributions to ionospheric chemistry as well as the chemical processing that occurs in the boundary layers between diffuse and dense interstellar clouds.
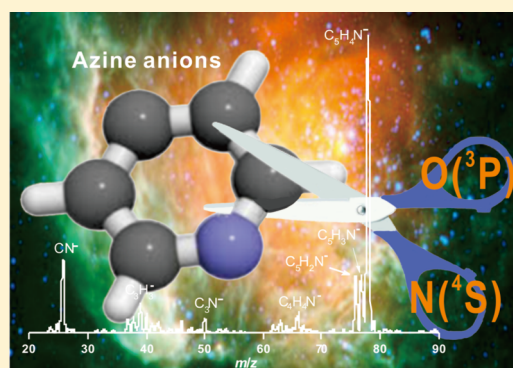
1. INTRODUCTION

Titan, the only natural satellite in our solar system with a dense atmosphere, has attracted increasing attention since the first encounter with the Cassini spacecraft in 2004.[1–11] The major component in Titan's upper atmosphere (~1000 km) is N_2 (>97%) with minor amounts of CH_4 (2%) and N-bearing organic species, as revealed by the ion neutral mass spectrometer (INMS) onboard the Cassini spacecraft.[11] The main initial ion production mechanisms in Titan's atmosphere are dissociation and ionization of nitrogen by solar wind, UV photons, and magnetospheric particles, generating very active species, including atomic nitrogen.[12] A large variety of neutral, cationic, and anionic species have been observed by the INMS together with the Cassini plasma spectrometer (CAPS),[13] indicating that the complex chemistry in Titan's upper atmosphere may play an important role in the formation of tholins.[2,14] Similar chemistry may have taken place in the atmosphere of early Earth before its buildup of oxygen 2.2×10^9 years ago.[15] The key precursors to heavy tholins are considered to be *aromatic*.[2,14] Furthermore, it was unexpected that negatively charged molecules, whose existence was not

previously considered, were widely observed by CAPS in high altitudes of Titan's atmosphere.[2,3,13,16–19] Although many studies have examined cationic-neutral reactions, few have focused on negatively charged reaction systems.[3,20–24] To the best of our knowledge, there are no kinetic studies or models on the reactions of atomic species with aromatic anions in Titan's upper atmosphere.

Our knowledge of astrochemistry has grown immensely over the last 80 years, albeit rather slowly in the beginning. The first interstellar molecule (CH) was detected in 1937,[25] and in the 25 subsequent years, only three additional species were detected by optical telescopes. Since the 1960s, microwave radio spectroscopy has led to many important discoveries starting with the detection of OH.[26] Today, nearly 200 interstellar and circumstellar species have been identified, including a wide variety of neutrals and positive ions.[27–29] The first negative ion, OCN^-, was identified in the icy mantles of interstellar dust grains.[30] However, gas phase negative ions were

not detected until 2006 and only six species, CN^-, C_3N^-, C_5N^-, C_4H^-, C_6H^-, and C_8H^-, have been confirmed to date.[31−37] The observation of interstellar negative ions is exciting, because it indicates that anion reactions could be important in the formation and distribution of species in the interstellar medium (ISM). N and O atoms show high interstellar atomic abundance.[28] In the interstellar environment, atomic species persist in more diffuse regions, while larger cyclic molecules and anions reside in dense molecular clouds. At the intersection of these regions, atoms chemically process larger molecules and anions. Most previous ion-atom studies have focused on reactions with cations.[38−40] However, little is known about the reactions of anions with N and O atoms, despite their abundant interstellar and atmospheric presence.[23,24,41−43]

Cyclic aromatic molecules are also ubiquitous throughout the interstellar medium.[2,44−47] Both neutral and ionic aromatic hydrocarbons and N-containing aromatic hydrocarbons have been suggested as the species whose visible absorption bands, the diffuse interstellar bands (DIBs),[48] have perplexed astrophysicists and chemists alike for nearly a century.[28,49−51] Additionally, N-containing aromatic hydrocarbons are important prebiotic molecules. For example, pyrimidine constitutes a key building block of nucleobases,[52] and the simple pyrimidine derivatives thymine, cytosine, and uracil are essential components of nucleic acids. The nucleobases have been formed in experimental simulations of Titan's atmosphere,[53] and the stability of their negative ions suggests their potential importance in these environments.[54] However, the specific identity of high mass anions in Titan's atmosphere must await higher resolution observations. Studies of the reactions of azine anions with interstellar and atmospheric species such as N and O atoms are thus important for gaining insight into the formation and persistence of complex molecules in these environments.

Studies involving reactions with N and O atoms are relatively rare, because the experiments are difficult to perform.[38] Recently, our group has successfully investigated the intriguing reactions of carbon chain anions (such as C_n^- and HC_n^-) as well as N-containing hydrocarbon chain anions (such as CH_2CN^-, CH_3CHCN^-, and $(CH_3)_2CCN^-$ with atomic $N(^4S)$ and $O(^3P)$).[23,24] The reactions of C_n^- with N atoms lead to the formation of N-containing carbon chain anions such as CN^-, C_3N^-, and C_5N^-, which are among the observed interstellar anions and are also observed in Titan's upper atmosphere.[3,31,35,36] Notably, the reaction rate constants of carbon chain anions with O atoms are approximately 1 order of magnitude larger than those with N atoms, and the neutral product CO is generated rather than C_nO^-.[24] The reactions of N-containing hydrocarbon chain anions with N and O atoms drew attention to spin-forbidden reactions and explored the influence of spin conservation and conversion on the reactions of interstellar species of high multiplicity such as $N(^4S)$ and $O(^3P)$.[23] N-containing hydrocarbon chain anions react rather slowly with N atoms (reaction rate constants on the order of 10^{-11} cm^3 s^{-1}), because the relative energy of the doublet-quartet crossing point is fairly close to the total energy of the entrance channel of the reactants. The O atom reactions for N-containing hydrocarbon chain anions are much faster (reaction rate constants $>7.0 \times 10^{-10}$ cm^3 s^{-1}), and they generate similar ionic products (for example, CN^-) as the N atom reactions.[23]

In this paper, the reactions of phenide ($C_6H_5^-$), pyridinide ($C_5H_4N^-$), 1,2-, 1,3-, and 1,4-diazinide ($C_4H_3N_2^-$) and 1,3,5-

triazinide ($C_3H_2N_3^-$) with ground state $N(^4S)$ and $O(^3P)$ atoms are studied at room temperature (Scheme 1). The major

Scheme 1. Deprotonated Species Studied in This Work
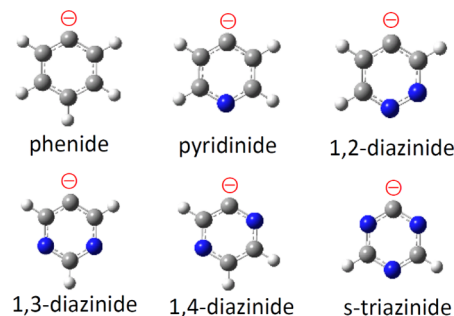
reaction channel of these azine anions with N and O atoms is associative electron detachment to produce electrons and neutral products. The reactions of N atoms with azine anions (reaction rate constants on the order of 10^{-10} cm^3 s^{-1}) are generally faster than those with the carbon chain anions.[23,24] Additionally, the reactions of azine anions with O atoms are ~2−5 times faster than those with N atoms and show complicated and intriguing ionic product patterns. Density functional theory (DFT) calculations are used to study the energies of the reactants, ion complexes, transition states, and products to examine reaction mechanisms in detail as well as to elucidate the spin conversion processes in the ion-atom reactions.

2. EXPERIMENTAL METHODS

Measurements of the reaction rate constants and product distributions were made using the tandem flowing afterglow-selected ion flow tube (FA-SIFT) at the University of Colorado, Boulder. This instrument has been described elsewhere,[55] and only the salient details for these experiments will be discussed here. Ions are generated using electron and chemical ionization methods in the source flow tube. A small flow of NH_3 entrained in helium buffer gas is passed over a rhenium filament to generate NH_2^-, which further reacts with azine molecules to form the deprotonated anions.

$$NH_2^- + HA \rightarrow NH_3 + A^- \qquad (1)$$

The anions are mass-selected with the SIFT quadrupole mass filter and injected into the reaction flow tube. They are then entrained in helium buffer gas (0.37 Torr, ~ 200 std cm^3 s^{-1}) at 298 K and thermalized by multiple collisions. The ion residence time in the flow tube is about 10 ms. The ion-neutral reaction is initiated by adding N or O atoms through an inlet positioned 70 cm upstream of the sampling orifice. Reactant and product ions are monitored with a quadrupole mass filter coupled with an electron multiplier. Microwave discharge flow techniques are used to generate N and O atoms in their ground states, which are well-established methods for studying the reactions of ions with atoms using the FA-SIFT.[23,24,56−62]

The N atoms are generated by flowing N_2 through a microwave discharge cavity operating at 30−60 W. The $O(^3P)$ atoms are formed by the subsequent titration of the N atoms with NO (4% NO in He) according to the reaction:[63,64]

$$N(^4S) + NO \rightarrow N_2 + O(^3P) \qquad (2)$$

Because of difficulties in measuring the absolute number densities of atoms, the total error in the rate constant measurements is estimated to be ±50%.

The main active species in the microwave discharge of N_2 is $N(^4S)$. Although appreciable concentrations of $N(^2D)$ and $N(^2P)$ metastable excited atoms have been found near the discharge plasma,[65,66] these

excited atoms, as well as N$_2$ ($^3\Sigma_u^+$), are destroyed within a few milliseconds.[67,68] The titration reaction shown in eq 2 is used to generate O(^{3}P), because this reaction is efficient.

Reaction 2 is one of the very few gas titration reactions with a visual end point.[69,70] Figure 1 shows the chemiluminescence of this titration
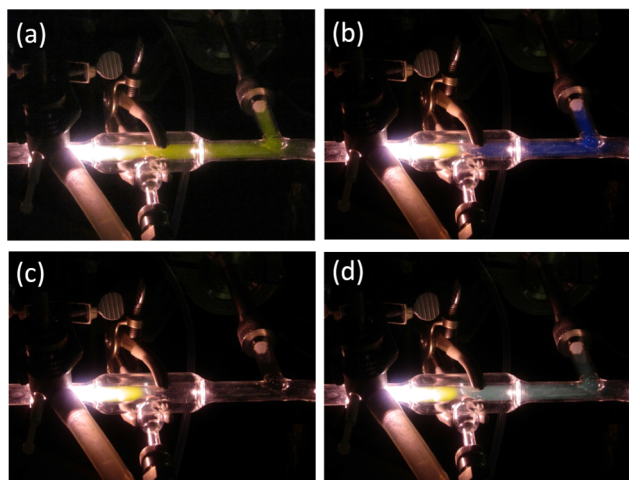

Figure 1. Titration processes involved in generating N and O atoms. (a) N atom flow (yellow luminescence) with pure N$_2$ flowing through the discharge region; (b) coexistence of N and O atoms (blue luminescence) due to the introduction of NO into the N atom flow; (c) titration end point with the existence of only O atoms (no color observed); (d) the coexistence of NO and O atoms after the titration end point (yellowish-green luminescence).

process. The pure N$_2$ flow is conducted through the microwave discharge region and ~1% of N$_2$ dissociates to N(^{4}S) atoms. The visible yellow chemiluminescence is due to excited N$_2$*, which is formed by the recombination of N atoms (Figure 1a):

$$N + N \rightarrow N_2^* \quad (3)$$

$$N_2^* \rightarrow N_2 + h\upsilon \quad (4)$$
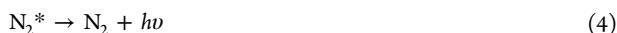
Addition of nitric oxide (NO) initiates the generation of O atom by reaction 2. The coexistence of N and O atom in the flow tube causes the blue chemiluminescence of NO* from the recombination of N + O,[71] shown in Figure 1b:

$$N + O \rightarrow NO^* \quad (5)$$

$$NO^* \rightarrow NO + h\upsilon \quad (6)$$

The intensity of the chemiluminescence decreases as the end point is approached until [NO]$_{added}$ = [N]$_0$; when chemiluminescence is no longer observed, [N] = 0 and [O] = [N]$_0$ (Figure 1c). Further addition of NO generates yellowish-green emission due to the excited ^{2}B$_1$ state of NO$_2$* (Figure 1d):

$$O + NO \rightarrow NO_2^* \quad (7)$$

$$NO_2^* \rightarrow NO_2 + h\upsilon \quad (8)$$

The generated NO$_2$ can react rapidly with O to form O$_2$ and NO. Thus, after the titration end point, the O atoms will be converted to O$_2$, catalyzed by NO, causing the partial recovery of ionic reactant signals. The removal of O atoms in this regime is very effective due to the relatively long distance in our apparatus between the discharge region and the flow tube.

3. CALCULATIONS

DFT calculations using the *Gaussian 09* program[72] are employed to study reactions of azine anions with N and O atoms. These calculations involve geometry optimization of various reaction intermediates and transition states. Transition state optimizations are

performed using either the Berny algorithm[73] or the synchronous transit-guided quasi-Newton (STQN) method.[74] For most cases, an initial estimated structure of the transition state is obtained through relaxed potential energy surface (PES) scans using an appropriate internal coordinate. Vibrational frequencies are calculated to confirm that the reaction intermediates have all positive frequencies and transition state species have only one imaginary frequency. Intrinsic reaction coordinate (IRC) calculations[75,76] are also performed so that a transition state connects two appropriate local minima in the reaction paths. The hybrid B3LYP exchange−correlation functional[77] is adopted. A Gaussian basis set 6-311++G(d,p) is used.[78,79] Test calculations indicate that basis set superposition error (BSSE) is negligible, and therefore BSSE is not taken into consideration. The zero-point vibration corrected energies (ΔE_{zpe}) are reported in this study. Cartesian coordinates, electronic energies, and vibrational frequencies for all of the optimized structures are available in the Supporting Information. The calculated energy for the reaction O$_2$ → ^{3}O + ^{3}O is 57.9 kcal mol^{-1} which agrees well with the experimental value of 58.7 kcal mol^{-1}. The calculated electron affinity for ^{3}O is 37.1 kcal mol^{-1}, which also agrees well with the experimental value of 33.7 kcal mol^{-1}. On the basis of these test calculations, the estimated uncertainty of the DFT calculations is ±4 kcal mol^{-1}.

4. RESULTS AND DISCUSSION

4.1. Generation of Atomic Species. The reactant ions phenide (C$_6$H$_5^-$), pyridinide (C$_5$H$_4$N$^-$), 1,2-, 1,3-, and 1,4-diazinide (C$_4$H$_3$N$_2^-$) and 1,3,5-triazinide (C$_3$H$_2$N$_3^-$) are allowed to react with N and O atoms. Figure 2 shows a typical
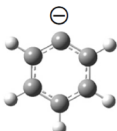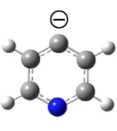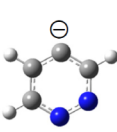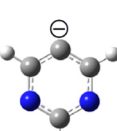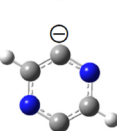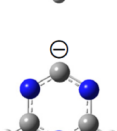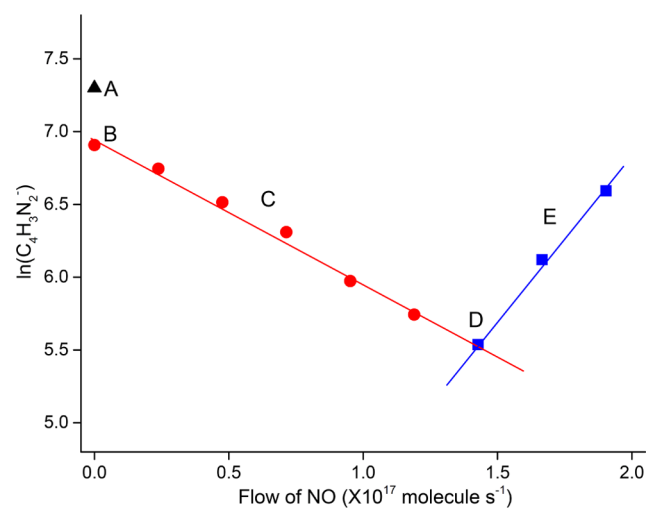

Figure 2. Titration plot for the reaction of 1,3-diazinide (C$_4$H$_3$N$_2^-$) with N and O atoms. Point A, microwave discharge off; point B, microwave discharge on; region C, coexistence of N and O atoms; point D, titration end point; region E, loss of O atom by reaction with NO.

titration plot, where the logarithm of the intensity of 1,3-diazinide (C$_4$H$_3$N$_2^-$) is plotted versus the flow of NO. At point A, molecular nitrogen is flowing into the system with the microwave discharge off; therefore, no reaction is evident. When the discharge is ignited, N atoms are formed, the ions react, and their intensity decreases to the lower value at point B. As NO is added to the system, N is converted to O, and the ion signal decreases due to the more rapid reaction of C$_4$H$_3$N$_2^-$ + O (region C). The intersection of the two lines at point D represents the end point of the titration; the flow of NO at this point is equal to both the N atom flow at the beginning of the titration as well as the O atom flow at the end point. Further

**Table 1. Reactions of Phenide Anion and Deprotonated Azine Anions with N and O Atoms Studied with FA-SIFT**

	Reactions with N (^{4}S)			Reactions with O (^{3}P)		
	AED[a]	Ionic Products	$k_{exp}(N)^{b}$ / 10^{-10} cm^3 s^{-1}	AED[a]	Ionic Products[d]	$k_{exp}(O)^{b}$ / 10^{-10} cm^3 s^{-1}
	1.0	N.D.[c]	1.8	0.9	$C_6H_3^-$ + H_2O (0.70) $C_5H_5^-$ + CO (0.15) HC_2^- + C_4H_4O (0.15)	9.0
	1.0	N.D.	1.3	0.9	CN^- + C_4H_4O (0.30) $C_5H_2N^-$ + H_2O (0.25) $C_5H_3N^-$ + OH (0.25) $C_3H_3^-$ + CO + HCN (0.08) C_3N^- + H_2O + C_2H_2 (0.05) $C_4H_4N^-$ + CO (0.07)	12
	1.0	N.D.	1.9	0.9	CN^- + C_3H_3NO (0.25) CCN^- + C_2H_3NO (0.15) C_4H^- + H_2O + N_2 (0.30) $OCCN^-$ + CH_3CN (0.30)	8.6
	1.0	N.D.	3.2	0.95	CN^- + C_3H_3NO (0.55) OCN^- + C_3H_3N (0.45)	12
	0.95	$C_4H_3N^-$ + N_2	2.5	0.8	CN^- + C_3H_3NO (0.55) HC_2N^- + C_2H_2NO (0.45)	7.5
	1.0	N.D.	3.1	0.85	OCN^- + $C_2H_2N_2$ (0.60) $OCNN^-$ + C_2H_2N (0.40)	7.2

[a]The branching fractions of associative electron detachment (AED) are obtained by comparing the decrease of the parent ion signal with the intensity of total product ion signals. [b]The total error is estimated to be ±50%. [c]Not detected. [d]Branching fractions for ionic product distributions are given in parentheses.

addition of NO beyond the end point, region E, causes the recovery of the ion signal, because O atoms are rapidly removed by reaction with NO to form NO_2 (eq 7). The ion loss, the atom flow rate, and other experimental parameters are used to determine the pseudo-first order reaction rate constants.

4.2. Reactivity of Azine Anions. *4.2.1. Reactions of N Atoms.* The rate constants and products for reactions of the azine anions with N (^{4}S) and O (^{3}P) atoms are summarized in Table 1. The dominant process for the reactions of azine anions with N atoms is associative electron detachment (AED) to form electrons and neutral products. There is no ionic product detected for the reactions of N atoms with $C_6H_5^-$, $C_5H_4N^-$, 1,2- and 1,3-$C_4H_3N_2^-$ and 1,3,5-$C_3H_2N_3^-$. The fact that AED dominates the chemistry between these species is relevant to Titan's atmospheric chemistry, as nitrogen incorporation has been shown to greatly influence the chemistry of polycyclic species in this environment.[80,81] Moreover, AED converts the identity of the negative charge carriers from ions to free electrons, which impacts the balance of these species. The only

minor ionic product detected from the reaction of 1,4-$C_4H_3N_2^-$ with N atoms is $C_4H_3N^-$, corresponding to the formation of neutral N_2, reaction 9:

$$C_4H_3N_2^- + N \rightarrow C_4H_3N^- + N_2 \qquad (9)$$
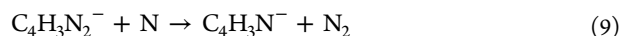
The rate constants for the reactions of azine anions with N atoms are larger than those of N-containing hydrocarbon chain anions with N atoms. For example, the reaction rate constant of $C_5H_4N^-$ with N atom is $1.3 \pm 0.7 \times 10^{-10}$ cm^3 molecule^{-1} s^{-1}, which is much larger than that of CH_2CN^- with N atom ($3.6 \pm 1.4 \times 10^{-11}$ cm^3 molecule^{-1} s^{-1}).[23]

A comparison of the reaction PESs of $C_5H_4N^-$ and CH_2CN^- with N atoms is shown in Figure 3. The most favorable way for the quartet ^{4}N atom to approach CH_2CN^- is at the terminal C atom of CH_2CN^- (Figure 3a), which shows a barrier of 1.1 kcal mol^{-1} higher than the energy of the reaction entrance channel. This barrier can be lowered to 0.5 kcal mol^{-1} (B3LYP/6-31+G(d,p)) via doublet-quartet PES crossing.[23] However, the existence of either a transition state or crossing point near the entrance channel of $CH_2CN^- + {}^4N$ makes this reaction slow.
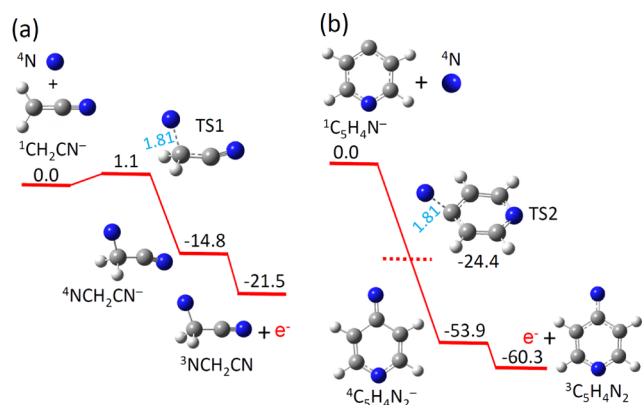
Figure 3. Quartet PESs for the reactions of (a) CH_2CN^- and (b) $C_5H_4N^-$ with N atoms. Note that the structure of TS2 is obtained by fixing the N–C distance to 1.81 Å and fully relaxing all other coordinates. The profiles are plotted for zero-point vibration corrected energies (E_{zpe}) relative to the energy of the entrance channel.

Additionally, our current level of theory has a maximum uncertainty of about ±4 kcal mol⁻¹, indicating that the small barrier calculated in this reaction may be slightly lower than the energy of the reactants, corresponding to the moderate reaction rate constant of $3.6 \pm 1.4 \times 10^{-11}$ cm³ s⁻¹. In contrast, the approach of ^4N atom to ground state $C_5H_4N^-$ is straightforward and barrierless with a significant energy release to form $NC_5H_4N^-$ (Figure 3b). The subsequent electron detachment leads to the formation of triplet neutral NC_5H_4N and an electron, shown in eq 10. The zero-point vibration corrected energies (E_{zpe}) are reported based on DFT calculations:

$$C_5H_4N^- + {}^4N \rightarrow {}^3NC_5H_4N + e^- \quad -60.3 \text{ kcal mol}^{-1} \quad (10)$$
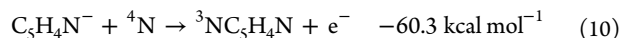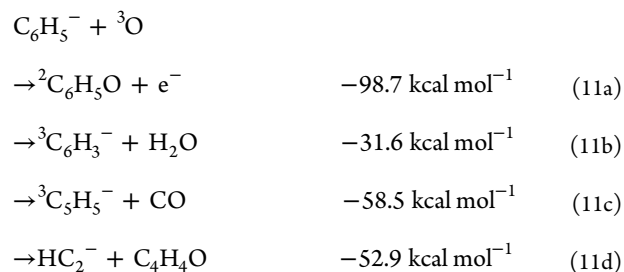
This comparison explains why the observed reaction rate constants of N atoms with deprotonated azine anions are faster than those with N-containing hydrocarbon chain anions. The direct association of ^4N atom to the deprotonated C atom site of the six-membered ring is found to be a common mechanism for the first attachment step of ^4N atom with deprotonated azine anions according to our DFT calculations.

It has been recently shown that the chemistry of negative ions is unexpectedly rich and complex in the upper atmosphere of Titan.[2,3,12,20,25−27] The rate constants of reactions of N atoms with azine anions reported here are thus crucial for the proper modeling of anionic reactions in Titan's atmosphere, whose environment mimics the evolution of the atmosphere of early Earth before its buildup of oxygen.[15] The observed high AED efficiency for the reactions of N atoms with both phenide and all azine anions is surprising. This observation, coupled with our former report of the high branching fractions of AED in the reactions of N atoms with carbon chain anions,[23,24] suggests a contribution of these processes to the electron-rich nature of Titan's upper atmosphere. Furthermore, subsequent dissociation of neutral products is possible following the AED, since these association reactions are highly exothermic (such as reaction 10). The reformation of N_2 molecules is feasible via the interaction of free N atoms with the skeleton N atoms to complete the nitrogen cycling in Titan's ionosphere. This argument is supported by the observation of the $C_4H_3N^- + N_2$ products from the reaction of 1,4-diazinide with N atoms (Table 1). Furthermore, the cleavage of the stable six-membered ring structure will enable the formation of small

N-containing hydrocarbon species, whose polymerization may contribute to the formation of Titan's tholins.[2,82,83]

4.2.2. Reaction of O Atoms with Phenide. The reactions of deprotonated azine anions with O atoms are complex, because various ionic products are observed experimentally in addition to AED (Table 1). However, the AED process is still dominant. The reaction rate constant of $C_6H_5^-$ with O atoms ($9.0 \pm 4.5 \times 10^{-10}$ cm³ molecule⁻¹ s⁻¹) is roughly 5 times faster than that with N atoms ($1.8 \pm 0.9 \times 10^{-10}$ cm³ molecule⁻¹ s⁻¹). The observed ionic products for this reaction are $C_6H_3^-$, $C_5H_5^-$, and HC_2^-, corresponding to the formation of neutral H_2O, CO, and C_4H_4O, respectively, shown in reaction 11:

$$C_6H_5^- + {}^3O$$

$$\rightarrow {}^2C_6H_5O + e^- \quad\quad -98.7 \text{ kcal mol}^{-1} \quad (11a)$$

$$\rightarrow {}^3C_6H_3^- + H_2O \quad\quad -31.6 \text{ kcal mol}^{-1} \quad (11b)$$

$$\rightarrow {}^3C_5H_5^- + CO \quad\quad -58.5 \text{ kcal mol}^{-1} \quad (11c)$$

$$\rightarrow HC_2^- + C_4H_4O \quad\quad -52.9 \text{ kcal mol}^{-1} \quad (11d)$$

According to our experimental observations, the generation of $C_6H_3^- + H_2O$ is the dominant ionic product channel (reaction 11b). The formation of carbon monoxide (reaction 11c) is not surprising since CO is very stable and the generation of CO has also been reported in the reactions of C_n^- and HC_n^- with O atoms.[24] The ionic product HC_2^- is the smallest member of the series HC_{2n}^-; the existence of the larger ions C_4H^-, C_6H^-, and C_8H^- in this family has been confirmed in the ISM.[32−34]

4.2.3. Reaction of O Atoms with Pyridinide. Several ionic products are observed from the reaction of $C_5H_4N^- + O$ including predominantly CN^-, $C_5H_2N^-$, and $C_5H_3N^-$, corresponding to the formation of neutral C_4H_4O, H_2O, and OH, respectively (Figure 4). Other low-abundance products such as $C_3H_3^-$, C_3N^-, and $C_4H_4N^-$ may arise from minor reaction channels. Comparing the reactions of $C_6H_5^-$ and $C_5H_4N^-$ with O atom, one can see that the reaction of N-containing $C_5H_4N^-$ with O atom favors the formation of N-containing ionic species as shown in Figure 4. The formation of

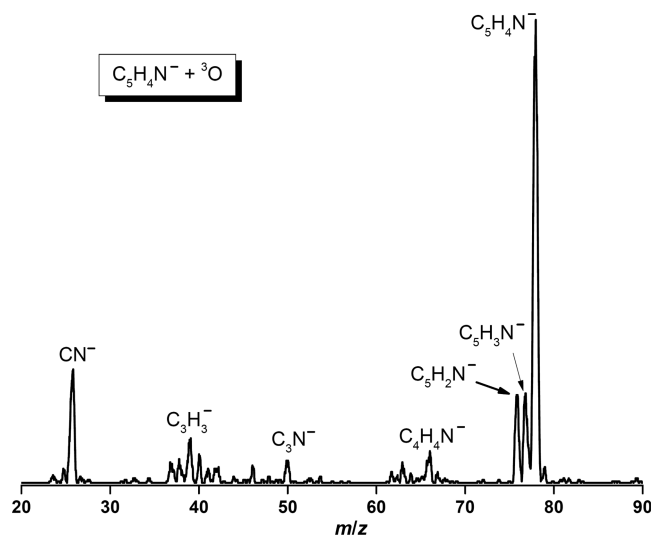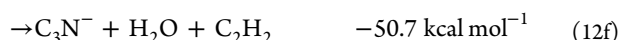**Figure 4.** Product distribution for the reaction of $C_5H_4N^-$ with O atoms is shown in this mass spectrum. Some very low intensity signals may arise from secondary reactions or system impurities.

these species is also observed for the reactions of other azine anions with O atoms (Table 1); these processes may be an important source of various N-containing species observed in Titan's atmosphere and in the ISM. The E_{zpe} of this reaction is studied by employing DFT calculations, shown in reaction 12:

$$C_5H_4N^- + {}^3O$$

$$\rightarrow {}^2C_5H_4NO + e^- \qquad\qquad -84.1 \text{ kcal mol}^{-1} \qquad (12a)$$

$$\rightarrow CN^- + {}^3CH_2COCHCH \qquad -31.1 \text{ kcal mol}^{-1} \qquad (12b)$$

$$\rightarrow C_5H_2N^- + H_2O \qquad\qquad -51.0 \text{ kcal mol}^{-1} \qquad (12c)$$

$$\rightarrow {}^2C_5H_3N^- + {}^2OH \qquad\qquad -11.1 \text{ kcal mol}^{-1} \qquad (12d)$$

$$\rightarrow C_3H_3^- + CO + HCN \qquad -52.4 \text{ kcal mol}^{-1} \qquad (12e)$$

$$\rightarrow C_3N^- + H_2O + C_2H_2 \qquad -50.7 \text{ kcal mol}^{-1} \qquad (12f)$$

$$\rightarrow C_4H_4N^- + CO \qquad\qquad -115 \text{ kcal mol}^{-1} \qquad (12g)$$

The formation of three major products by the reaction of $C_5H_4N^-$ with ${}^3O$ atom on the triplet PES is shown in Figure 5.

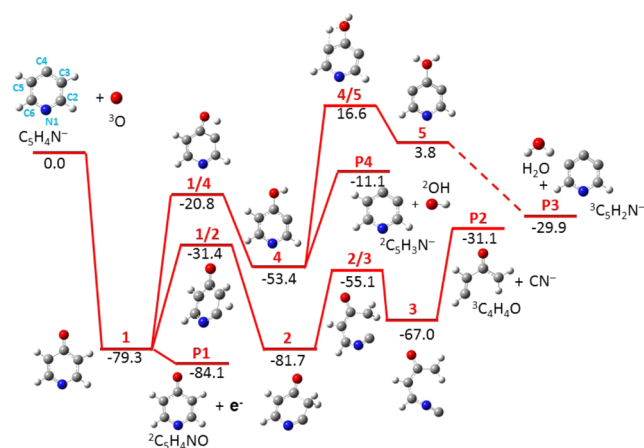**Figure 5.** PES for the reaction of $C_5H_4N^-$ with ${}^3O$ on the triplet surface. The profiles are plotted for zero-point vibration corrected energies (E_{zpe}) relative to the energy of the entrance channel. The E_{zpe} is given in kcal mol^{-1}. The intermediates and transition states are denoted in bold as n and $n1/n2$, respectively, and the products are denoted in bold as Pn.

The $C_5H_4N^-$ is deprotonated at the C4 site, which has been verified by our former studies of its photoelectron spectrum.[84] The interaction of ${}^3O$ atom with the C4 site of the $C_5H_4N^-$ is barrierless and associated with a large energy release (-79.3 kcal mol^{-1}) to form intermediate **1**. An electron can be lost from **1** to generate the neutral doublet ${}^2C_5H_4NO$. This AED process is highly exothermic (-84.1 kcal mol^{-1}) and the product branching fraction is experimentally estimated to be ~0.9 (Table 1). From intermediate **1**, hydrogen atom transfer occurs either from the C3 atom to the oxygen or from the C2 to the C3 atom, leading to the formation of ${}^3C_5NH_3-OH$ (**4**) or c-${}^3CH_2COCHCHNC$ (**2**), respectively. From intermediate **2**, the cleavage of the six-membered ring is feasible at the C2$-$C3 bond and the formation of the CN^- product can be achieved (**2** $\rightarrow$ **2/3** $\rightarrow$ **3** $\rightarrow$ **P2**). The generation of CN^- + ${}^3C_4H_4O$ (**P2**) is also a barrierless reaction channel, although the reaction to form **P2** (-31.1 kcal mol^{-1}) is much less

exothermic than that to form **P1**. The loss of the ${}^2OH$ radical from **4** can generate the experimentally observed ${}^2C_5H_3N^-$ (**4** $\rightarrow$ **P4**). Unlike the formation of the ${}^2OH$ radical, the production of H_2O requires a second hydrogen atom transfer (**4** $\rightarrow$ **4/5** $\rightarrow$ **5** $\rightarrow$ **P3**) with a high barrier of 16.6 kcal mol^{-1} (transition state **4/5**) and thus is impossible on the triplet potential energy surface. This calculated high barrier on the triplet PES for the formation of H_2O + ${}^3C_5H_2N^-$ does not agree with our experimental observations; therefore, we have pursued this calculation in greater detail and discuss our findings below.

The reaction is barrierless and more exothermic to form the singlet products H_2O + $C_5H_2N^-$ from the triplet reactants via a crossing point as shown in Figures 6 and 7. This crossing point

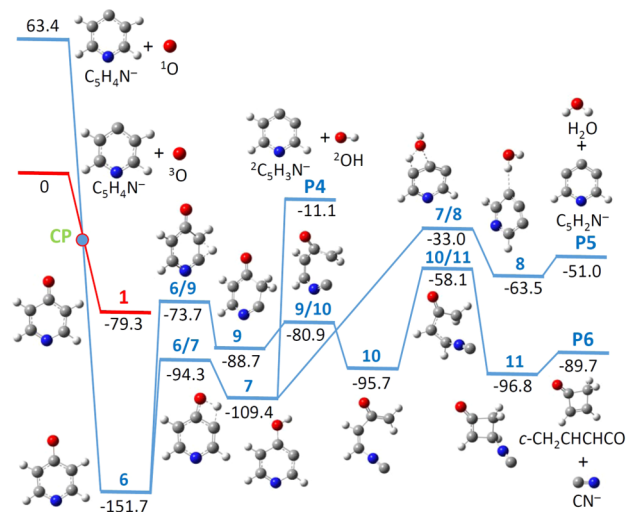**Figure 6.** PES for the reaction of $C_5H_4N^-$ with ${}^1O$ on the singlet surface. The profiles are plotted for zero-point vibration corrected energies (E_{zpe}) relative to the energy of the entrance channel. The E_{zpe} is given in kcal mol^{-1}. The intermediates and transition states are denoted in bold as n and $n1/n2$, respectively, and the products are denoted in bold as Pn. CP designates the crossing point for the singlet and triplet surfaces.

can only occur between the reactants and the first encounter complex (intermediate **6**), because the singlet intermediate **6** possesses a very similar structure to the triplet intermediate **1**,
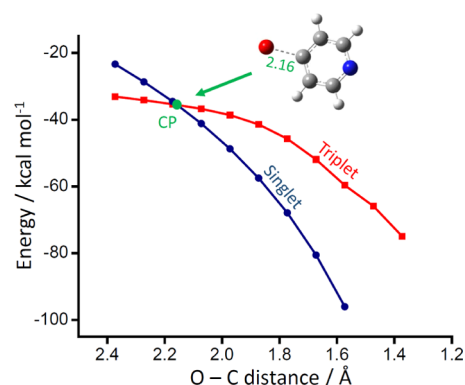

Figure 7. Relaxed PES scan of the entrance channel of $C_5H_4N^-$ with O for the singlet and triplet spin states. The singlet–triplet crossing point is determined to possess the same structure and energy on both singlet and triplet PESs.

but is 72.4 kcal mol^{-1} more stable than **1** (Figure 6). Starting from **6**, the process to generate **P5** (H$_2$O + C$_5$H$_2$N$^-$) similarly involves the consecutive hydrogen atom transfers (**6 → 6/7 → 7 → 7/8 → 8 → P5**) and the highest barrier (transition state **7/8**) of this reaction pathway is −33.0 kcal mol^{-1} lower in energy than the triplet reactants. In the reaction of C$_5$H$_4$N$^-$ + O, the major reaction channel is AED, which has a branching fraction of 90% (Table 1). The ionic product channel that generates C$_5$H$_2$N$^-$ + H$_2$O via the crossing between the singlet and triplet potential energy surfaces contributes a branching fraction of only 2.5%. This value corresponds to a rate constant of 3.0 × 10^{-11} cm^3 s^{-1}, which is 40 times lower than the total reaction rate constant for the C$_5$H$_4$N$^-$ + O reaction. The products ^{2}C$_5$H$_3$N$^-$ + ^{2}OH (**P4**) and c-C$_4$H$_4$O + CN$^-$ (**P6**) can also be formed from the singlet PES without barriers as shown in Figure 6. The formation of H$_2$O + C$_5$H$_2$N$^-$ is more kinetically favorable than C$_5$H$_3$N$^-$ + OH on the singlet PES. However, C$_5$H$_3$N$^-$ + OH can also be generated from the triplet PES as shown in Figure 5, which gives a reasonable explanation for the observed similar intensities of C$_5$H$_2$N$^-$ and C$_5$H$_3$N$^-$ in Figure 4. The formation of CN$^-$ + C$_4$H$_4$O (triplet **P2** in Figure 5 and singlet **P6** in Figure 6) is the most favorable reaction pathway on either the singlet or triplet PES, which agrees well with the experimentally observed highest intensity signal from CN$^-$. The formation of C$_4$H$_4$N$^-$, C$_3$H$_3$$^-$, and C$_3N^-$ is thermodynamically favorable as shown in reactions 12e−12g, and the low ion signals (Figure 4) indicate the probable existence of relatively higher kinetic barriers on their reaction pathways.

4.2.4. Reactions of O Atoms with Diazinides. Similar to the reactions of N-containing hydrocarbon chain anions with O atoms, the ionic CN$^-$ product is observed for all reactions of deprotonated diazine anions with O atoms (see Table 1 for details). However, in the reactions of N-containing hydrocarbon chain anions with O atoms, CN$^-$ is the only major ionic product,[23] while there are complex product patterns from the reactions of deprotonated diazine anions with O atoms. Four ionic products are observed for the reaction of 1,2-C$_4$H$_3$N$_2$$^-$ with O atoms, corresponding to CN$^-$, CCN$^-$, C$_4$H$^-$, and OCCN$^-$, respectively. Among these anion products, C$_4$H$^-$ and OCCN$^-$ are dominant, and correspond to the formation of the neutral species H$_2$O + N$_2$ and CH$_3$CN, respectively. For the reaction of 1,3-C$_4$H$_3$N$_2$$^-$ + O, two ionic products, CN$^-$ and OCN$^-$, are detected with similar intensities. The reaction of 1,4-C$_4$H$_3$N$_2$$^-$ + O leads to the generation of CN$^-$ and HC$_2$N$^-$ with the ionic branching fractions 0.55 and 0.45, respectively. The reaction of 1,3-C$_4$H$_3$N$_2$$^-$ with O atoms is studied in detail using DFT calculations. The parent neutral of 1,3-C$_4$H$_3$N$_2$$^-$ is 1,3-diazine (pyrimidine), which is an important prebiotic molecule.[52] The reaction rate constant for the reaction of 1,3-C$_4$H$_3$N$_2$$^-$ with ^{3}O atom is 1.2 ± 0.6 × 10^{-9} cm^3 s^{-1}. With AED as the major reaction channel, ionic products observed in this reaction are OCN$^-$ and CN$^-$, reaction 13:

$$C_4H_3N_2^- + {}^3O$$

$$\rightarrow {}^2C_4H_3N_2O + e^- \qquad -78.8\ \text{kcal mol}^{-1} \qquad (13a)$$

$$\rightarrow CN^- + {}^3C_3H_3NO \qquad -41.4\ \text{kcal mol}^{-1} \qquad (13b)$$

$$\rightarrow OCN^- + {}^3C_3H_3N \qquad -34.5\ \text{kcal mol}^{-1} \qquad (13c)$$
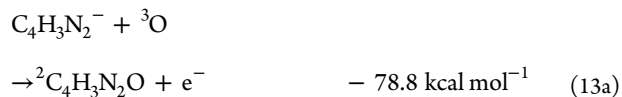
Figure 8 shows the reaction of 1,3-C$_4$H$_3$N$_2$$^-$ with O atoms on the triplet PES. The initial step for the combination of 1,3-
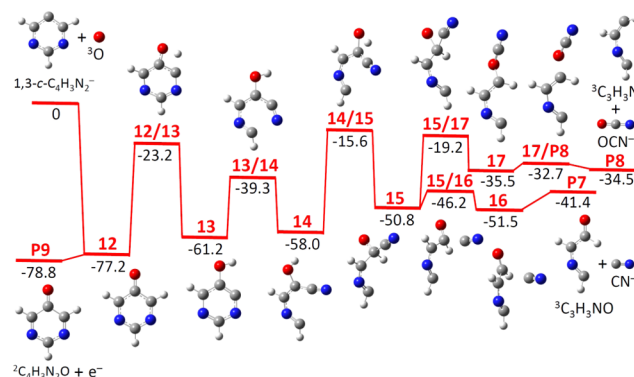

Figure 8. PES for the reaction of 1,3-C$_4$H$_3$N$_2$$^-$ with ^{3}O on the triplet surface. The profiles are plotted for zero-point vibration corrected energies (E_{zpe}) relative to the energy of the entrance channel. The E_{zpe} is given in kcal mol^{-1}. The intermediates and transition states are denoted in bold as *n* and *n1/n2*, respectively, and the products are denoted in bold as *Pn*.

C$_4$H$_3$N$_2$$^-$ with ground state O atoms is straightforward to form the encounter complex (intermediate **12**, − 77.2 kcal mol^{-1}). The binding energy of this process is sufficient for either the AED channel to generate C$_4$H$_3$N$_2$O + e$^-$ (**P9**, − 78.8 kcal mol^{-1}) or the following complicated hydrogen atom transfer and ring-opening processes (**12 → 12/13 → 13 → 13/14 → 14 → 14/15 → 15**). From intermediate **15**, the loss of the CN moiety will lead to the products CN$^-$ + ^{3}C$_3$H$_3$NO (**15 → 15/16 → 16 → P7**), while rearrangement of the O atom inserted into the carbon chain constructs a long-chain structure containing an OCN group (intermediate **17**). The breaking of the O−C bond and the consecutive loss of the OCN moiety from the terminal chain structure results in the formation of OCN$^-$ + ^{3}C$_3$H$_3$N (**P8**, − 34.5 kcal mol^{-1}). The generation of the singlet products, e.g., OCN$^-$ + C$_3$H$_3$N and CN$^-$ + C$_3$H$_3$NO may also be possible via a crossing point between the triplet and the singlet PESs. Note that both OCN$^-$ and CN$^-$ are important negatively charged interstellar species.

4.2.5. Reaction of O Atoms with 1,3,5-Triazinide. The ionic products observed for the reaction of 1,3,5-C$_3$H$_2$N$_3$$^-$ with O atoms are OCNN$^-$ and OCN$^-$. The CN$^-$ product which has been observed in reactions of other azine anions + O atoms is not detected in this reaction. The reaction channels observed are summarized in reaction 14:

$$C_3H_2N_3^- + {}^3O$$

$$\rightarrow {}^2C_3H_2N_3O + e^- \qquad -74.4\ \text{kcal mol}^{-1} \qquad (14a)$$

$$\rightarrow OCN^- + {}^3C_2H_2N_2 \qquad -60.8\ \text{kcal mol}^{-1} \qquad (14b)$$

$$\rightarrow {}^2OCNN^- + {}^2C_2H_2N \qquad -35.9\ \text{kcal mol}^{-1} \qquad (14c)$$

As shown in Figure 9, the direct association of 1,3,5-C$_3$H$_2$N$_3$$^-$ with an O atom forms the triplet intermediate **18** (−92.2 kcal mol^{-1}) that can undergo electron detachment, and the products ^{2}C$_3$H$_2$N$_3$O + e$^-$ (**P12**) are 74.4 kcal mol^{-1} below the total energy of the reactants. From intermediate **18**, the formation of intermediate **20** with a CH$_2$ moiety in the six-membered ring can be realized via consecutive hydrogen atom transfers over the ring skeleton (**18 → 18/19 → 19 → 19/20 → 20**). This hydrogen atom transfer process allows the next ring-opening step to form the OCNN moiety (**20 → 20/21 → 21**). The direct elimination of OCNN from intermediate **21** leads to the
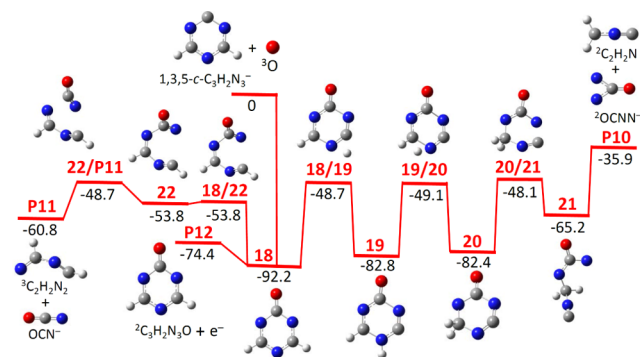
Figure 9. PES for the reaction of 1,3,5-$C_3H_2N_3^-$ with ^3O on the triplet surface. The profiles are plotted for zero-point vibration corrected energies (E_{zpe}) relative to the energy of the entrance channel. The E_{zpe} is given in kcal mol^{-1}. The intermediates and transition states are denoted in bold as *n* and *n1/n2*, respectively, and the products are denoted in bold as ***Pn***.

final products, $^2OCNN^- + {}^2C_2H_2N$ (**P10**). On the other hand, the direct cleavage of the six-membered ring structure may occur from **18**, leading to the open ring intermediate **22** with the formation of an OCN group. The generation of OCN$^-$ + $^3C_2H_2N_2$ is straightforward from **22** with a barrier 48.7 kcal mol^{-1} lower in energy than the initial reactants. According to our experimental observations, AED is the dominant process and the intensity of the OCN$^-$ signal is larger than that of $^2OCNN^-$ (Table 1), which agrees well with calculations on the triplet PES. Although spin conversion might be possible during the formation of the ionic products, the transfer between PESs of different multiplicities is usually the rate-limiting step. Therefore, it is reasonable to consider the reaction pathways that occur within the PES of the same multiplicity to be the major channels, given that the formation of products are exothermic and barrierless. The computed results complement the experimental observations well for the reaction of 1,3,5-$C_3H_2N_3^-$ with O atoms.

5. CONCLUSIONS

Gas phase ion-atom reactions of deprotonated azines with N and O atoms are studied both experimentally and computationally. From the boundary layers between diffuse and dense interstellar clouds, to the atmospheres of early Earth and satellites such as Titan, these reactions provide important information regarding the chemical processing of atomic and molecular species in these environments. In all cases, the major reaction channel is AED, which transfers negative charge from anions to free electrons. The reactions of the azine anions with N atoms exhibit larger reaction rate constants when compared to those of N-containing hydrocarbon chain anions, because the association of N atom with the azine anions is straightforward and barrierless on the quartet PES. There are no ionic products observed for most of the reactions of the azine anions with N atoms. The only ionic product observed is $C_4H_3N^-$, which arises from the reaction of 1,4-$C_4H_3N_2^-$ + N and corresponds to the formation of neutral N$_2$; this process provides a route for the regeneration of molecular nitrogen in these environments.[80]

The reaction rate constants of azine anions with O atoms are near the collisional limit;[85,86] these reactions are more exothermic and faster than the corresponding reactions with N atoms. This behavior parallels our previous studies of the

reactions of H atoms in which reactivity correlates with exothermicity.[87] This result may reflect the fact that, for similar processes, more exothermic reactions tend to have lower energy barriers, and therefore a great number of states leading to reaction. In addition, more complex product patterns are observed for the O atom reactions. The ionic product CN$^-$ can be observed for all studied reactions of azine anions with O atoms except for the 1,3,5-$C_3H_2N_3^-$ + O reaction; the latter only generates OCNN$^-$ and OCN$^-$. The mechanisms for the formation of various ionic products via the reaction of azine anions with O atoms are studied in detail using DFT calculations. The spin conversion process is found to be essential to the formation of $C_5H_2N^- + H_2O$ from the reaction of $C_5H_4N^-$ with O atoms, while many other ionic products of azine anions + O reactions can be formed directly from triplet PESs without barriers.

The temperatures in the ISM and in Titan's atmosphere are much lower than 298 K. Since the reaction rate constants of azine anions with O atoms are close to the capture limit, no strong temperature dependence is expected. However, in the case of N atoms, strong temperature effects are possible;[88] thus temperature variable experimental studies are highly desired for providing important benchmarks for theoretical assessments.

The ionic products observed herein (CN$^-$, C_3N^-, C_2H^-, C_4H^-, and OCN$^-$) are important N-containing species that exist in Titan's atmosphere and the ISM. These reactions illuminate the complex chemistry between N and O atoms and azine anions, and synthesize other known interstellar and atmospheric molecules in the process. This work uncovers important mechanisms and, coupled with additional observations and modeling, may shed light on the identities, abundances, and roles of negative ions in an array of astrochemical environments.

■ ASSOCIATED CONTENT

ⓢ Supporting Information

The Supporting Information is available free of charge on the ACS Publications website at DOI: 10.1021/jacs.5b06089.

Cartesian coordinates and zero point corrected energies for all of the optimized structures. (PDF)

■ AUTHOR INFORMATION

Corresponding Authors

*zhechen.wang@colorado.edu

*veronica.bierbaum@colorado.edu

Present Address

#Department of Physics, University of Auckland, Private Bag 92019, Auckland, New Zealand.

Notes

The authors declare no competing financial interest.

■ ACKNOWLEDGMENTS

■ REFERENCES

(1) Vuitton, V.; Yelle, R. V.; Anicich, V. G. *Astrophys. J.* **2006**, *647*, L175.

(2) Waite, J. H., Jr.; Young, D. T.; Cravens, T. E.; Coates, A. J.; Crary, F. J.; Magee, B.; Westlake, J. *Science* **2007**, *316*, 870.

(3) Vuitton, V.; Lavvas, P.; Yelle, R. V.; Galand, M.; Wellbrock, A.; Lewis, G. R.; Coates, A. J.; Wahlund, J. E. *Planet. Space Sci.* **2009**, *57*, 1558.

(4) Demarais, N. J.; Yang, Z.; Snow, T. P.; Bierbaum, V. M. *Struct. Chem.* **2013**, *24*, 1957.

(5) Vuitton, V.; Yelle, R. V.; McEwan, M. J. *Icarus* **2007**, *191*, 722.

(6) Lavvas, P.; Yelle, R. V.; Koskinen, T.; Bazin, A.; Vuitton, V.; Vigren, E.; Galand, M.; Wellbrock, A.; Coates, A. J.; Wahlund, J. E.; Crary, F. J.; Snowden, D. *Proc. Natl. Acad. Sci. U. S. A.* **2013**, *110*, 2729.

(7) Gautier, T.; Carrasco, N.; Buch, A.; Szopa, C.; Sciamma-O'Brien, E.; Cernogora, G. *Icarus* **2011**, *213*, 625.

(8) Wilson, E. H.; Atreya, S. K. *J. Phys. Chem. A* **2009**, *113*, 11221.

(9) Coustenis, A.; Hirtzig, M. *Res. Astron. Astrophys.* **2009**, *9*, 249.

(10) Vuitton, V.; Yelle, R. V.; Cui, J. *J. Geophys. Res.* **2008**, *113*, E05007.

(11) Waite, J. H.; Niemann, H.; Yelle, R. V.; Kasprzak, W. T.; Cravens, T. E.; Luhmann, J. G.; McNutt, R. L.; Ip, W. H.; Gell, D.; De La Haye, V.; Muller-Wordag, I.; Magee, B.; Borggren, N.; Ledvina, S.; Fletcher, G.; Walter, E.; Miller, R.; Scherer, S.; Thorpe, R.; Xu, J.; Block, B.; Arnett, K. *Science* **2005**, *308*, 982.

(12) Geppert, W. D.; Larsson, M. *Chem. Rev.* **2013**, *113*, 8872.

(13) Young, D. T.; Berthelier, J. J.; Blanc, M.; Burch, J. L.; Coates, A. J.; Goldstein, R.; Grande, M.; Hill, T. W.; Johnson, R. E.; Kelha, V.; McComas, D. J.; Sittler, E. C.; Svenes, K. R.; Szego, K.; Tanskanen, P.; Ahola, K.; Anderson, D.; Bakshi, S.; Baragiola, R. A.; Barraclough, L.; Black, R. K.; Bolton, S.; Booker, T.; Bowman, R.; Casey, P.; Crary, F. J.; Delapp, D.; Dirks, G.; Eaker, N.; Funsten, H.; Furman, J. D.; Gosling, J. T.; Hannula, H.; Holmlund, C.; Huomo, H.; Illiano, J. M.; Jensen, P.; Johnson, M. A.; Linder, D. R.; Luntama, T.; Maurice, S.; McCabe, K. P.; Mursula, K.; Narheim, B. T.; Nordholt, J. E.; Preece, A.; Rudzki, J.; Ruitberg, A.; Smith, K.; Szalai, S.; Thomsen, M. F.; Viherkanto, K.; Vilppola, J.; Vollmer, T.; Wahl, T. E.; Wuest, M.; Ylikorpi, T.; Zinsmeyer, C. *Space Sci. Rev.* **2004**, *114*, 1.

(14) Atreya, S. *Science* **2007**, *316*, 843.

(15) Pavlov, A. A.; Hurtgen, M. T.; Kasting, J. F.; Arthur, M. A. *Geology* **2003**, *31*, 87.

(16) Shebanits, O.; Wahlund, J. E.; Mandt, K.; Agren, K.; Edberg, N. J. T.; Waite, J. H. *Planet. Space Sci.* **2013**, *84*, 153.

(17) Wellbrock, A.; Coates, A. J.; Jones, G. H.; Lewis, G. R.; Waite, J. H. *Geophys. Res. Lett.* **2013**, *40*, 4481.

(18) Agren, K.; Edberg, N. J. T.; Wahlund, J. E. *Geophys. Res. Lett.* **2012**, *39*, L10201.

(19) Coates, A. J.; Wellbrock, A.; Lewis, G. R.; Jones, G. H.; Young, D. T.; Crary, F. J.; Waite, J. H. *Planet. Space Sci.* **2009**, *57*, 1866.

(20) Biennier, L.; Carles, S.; Cordier, D.; Guillemin, J. C.; Le Picard, S. D.; Faure, A. *Icarus* **2014**, *227*, 123.

(21) Sebastianelli, F.; Carelli, F.; Gianturco, F. A. *Chem. Phys.* **2012**, *398*, 199.

(22) Carles, S.; Adjali, F.; Monnerie, C.; Guillemin, J. C.; Le Garrec, J. L. *Icarus* **2011**, *211*, 901.

(23) Yang, Z.; Eichelberger, B.; Martinez, O., Jr.; Stepanovic, M.; Snow, T. P.; Bierbaum, V. M. *J. Am. Chem. Soc.* **2010**, *132*, 5812.

(24) Eichelberger, B.; Snow, T. P.; Barckholtz, C.; Bierbaum, V. M. *Astrophys. J.* **2007**, *667*, 1283.

(25) Swings, P.; Rosenfeld, L. *Astrophys. J.* **1937**, *86*, 483.

(26) Weinreb, S.; Barrett, A. H.; Henry, J. C.; Meeks, M. L. *Nature* **1963**, *200*, 829.

(27) Herbst, E. *Chem. Soc. Rev.* **2001**, *30*, 168.

(28) Snow, T. P.; Bierbaum, V. M. *Annu. Rev. Anal. Chem.* **2008**, *1*, 229.

(29) Petrie, S.; Bohme, D. K. *Mass Spectrom. Rev.* **2007**, *26*, 258.

(30) Soifer, B. T.; Puetter, R. C.; Russell, R. W.; Willner, S. P.; Harvey, P. M.; Gillett, F. C. *Astrophys. J.* **1979**, *232*, L53.

(31) Agundez, M.; Cernicharo, J.; Guelin, M.; Kahane, C.; Roueff, E.; Klos, J.; Aoiz, F. J.; Lique, F.; Marcelino, N.; Goicoechea, J. R.; Garcia, M. G.; Gottlieb, C. A.; McCarthy, M. C.; Thaddeus, P. *Astron. Astrophys.* **2010**, *517*, L2.

(32) Cernicharo, J.; Guelin, M.; Agundez, M.; Kawaguchi, K.; McCarthy, M.; Thaddeus, P. *Astron. Astrophys.* **2007**, *467*, L37.

(33) McCarthy, M. C.; Gottlieb, C. A.; Gupta, H.; Thaddeus, P. *Astrophys. J.* **2006**, *652*, L141.

(34) Brunken, S.; Gupta, H.; Gottlieb, C. A.; McCarthy, M. C.; Thaddeus, P. *Astrophys. J.* **2007**, *664*, L43.

(35) Cernicharo, J.; Guelin, M.; Agundez, M.; McCarthy, M. C.; Thaddeus, P. *Astrophys. J.* **2008**, *688*, L83.

(36) Thaddeus, P.; Gottlieb, C. A.; Gupta, H.; Bruenken, S.; McCarthy, M. C.; Agundez, M.; Guelin, M.; Cernicharo, J. *Astrophys. J.* **2008**, *677*, 1132.

(37) Herbst, E. *Nature* **1981**, *289*, 656.

(38) Scott, G. B. I.; Fairley, D. A.; Milligan, D. B.; Freeman, C. G.; McEwan, M. J. *J. Phys. Chem. A* **1999**, *103*, 7470.

(39) Scott, G. B. I.; Fairley, D. A.; Freeman, C. G.; McEwan, M. J.; Anicich, V. G. *J. Phys. Chem. A* **1999**, *103*, 1073.

(40) Scott, G. B. I.; Fairley, D. A.; Freeman, C. G.; McEwan, M. J.; Anicich, V. G. *J. Chem. Phys.* **1998**, *109*, 9010.

(41) Ard, S. G.; Melko, J. J.; Jiang, B.; Li, Y.; Shuman, N. S.; Guo, H.; Viggiano, A. A. *J. Chem. Phys.* **2013**, *139*, 144302.

(42) Bierbaum, V. M. In *Molecular Universe*; Cernicharo, J., Bachiller, R., Eds.; Cambridge University Press: Cambridge, U.K., 2011; p 383.

(43) Yang, Z.; Snow, T. P.; Bierbaum, V. M. *Phys. Chem. Chem. Phys.* **2010**, *12*, 13091.

(44) Snow, T. P.; Le Page, V.; Keheyan, Y.; Bierbaum, V. M. *Nature* **1998**, *391*, 259.

(45) Bohme, D. K. *Chem. Rev.* **1992**, *92*, 1487.

(46) Candian, A.; Sarre, P. J. *Mon. Not. R. Astron. Soc.* **2015**, *448*, 2960.

(47) Tian, M.; Liu, B. S.; Hammonds, M.; Wang, N.; Sarre, P. J.; Cheung, A. S. C. *Phys. Chem. Chem. Phys.* **2012**, *14*, 6603.

(48) Herbst, E.; van Dishoeck, E. F. *Annu. Rev. Astron. Astrophys.* **2009**, *47*, 427.

(49) Sarre, P. J. *J. Mol. Spectrosc.* **2006**, *238*, 1.

(50) Sarre, P. J.; Miles, J. R.; Scarrott, S. M. *Science* **1995**, *269*, 674.

(51) Sarre, P. J. *Nature* **1991**, *351*, 356.

(52) Landera, A.; Mebel, A. M. *J. Am. Chem. Soc.* **2013**, *135*, 7251.

(53) Horst, S. M.; Yelle, R. V.; Buch, A.; Carrasco, N.; Cernogora, G.; Dutuit, O.; Quirico, E.; Sciamma-O'Brien, E.; Smith, M. A.; Somogyi, A.; Szopa, C.; Thissen, R.; Vuitton, V. *Astrobiology* **2012**, *12*, 809.

(54) Cole, C. A.; Demarais, N. J.; Yang, Z.; Snow, T. P.; Bierbaum, V. M. *Astrophys. J.* **2013**, *779*, 181.

(55) Van Doren, J. M.; Barlow, S. E.; DePuy, C. H.; Bierbaum, V. M. *Int. J. Mass Spectrom. Ion Processes* **1987**, *81*, 85.

(56) Demarais, N. J.; Yang, Z. B.; Snow, T. P.; Bierbaum, V. M. *Astrophys. J.* **2014**, *784*, 25.

(57) Thomsen, D. L.; Reece, J. N.; Nichols, C. M.; Hammerum, S.; Bierbaum, V. M. *J. Am. Chem. Soc.* **2013**, *135*, 15508.

(58) Nichols, C. M.; Yang, Z.; Bierbaum, V. M. *Int. J. Mass Spectrom.* **2013**, *353*, 1.

(59) Garver, J. M.; Yang, Z.; Nichols, C. M.; Worker, B. B.; Gronert, S.; Bierbaum, V. M. *Int. J. Mass Spectrom.* **2012**, *316*, 244.

(60) Yang, Z.; Cole, C. A.; Martinez, O., Jr.; Carpenter, M. Y.; Snow, T. P.; Bierbaum, V. M. *Astrophys. J.* **2011**, *739*, 193.

(61) Martinez, O.; Sanchez, J. C.; Ard, S. G.; Li, A. Y.; Melko, J. J.; Shuman, N. S.; Guo, H.; Viggiano, A. A. *J. Chem. Phys.* **2015**, *142*, 54305.

(62) Cox, R. M.; Kim, J.; Armentrout, P. B.; Bartlett, J.; VanGundy, R. A.; Heaven, M. C.; Ard, S. G.; Melko, J. J.; Shuman, N. S.; Viggiano, A. A. *J. Chem. Phys.* **2015**, *142*, 134307.

(63) Lee, J. H.; Michael, J. V.; Payne, W. A.; Stief, L. J. *J. Chem. Phys.* **1978**, *69*, 3069.

(64) Clyne, M. A. A.; McDermid, I. S. *J. Chem. Soc., Faraday Trans. 1* **1975**, *71*, 2189.

(65) Foner, S. N.; Hudson, R. L. *J. Chem. Phys.* **1962**, *37*, 1662.

(66) Lin, C. L.; Kaufman, F. *J. Chem. Phys.* **1971**, *55*, 3760.

(67) Meyer, J. A.; Setser, D. W.; Stedman, D. H. *J. Phys. Chem.* **1970**, *74*, 2238.

(68) Young, R. A.; St. John, G. A. *J. Chem. Phys.* **1968**, *48*, 895.

(69) Kaufman, F. *Prog. React. Kinet. Mech.* **1961**, *1*, 1.

(70) Brocklehurst, B.; Jennings, K. R. *Prog. React. Kinet.* **1967**, *4*, 1.

(71) Gatz, C. R.; Young, R. A.; Sharpless, R. L. *J. Chem. Phys.* **1963**, *39*, 1234.

(72) Frisch, M. J.; Trucks, G. W.; Schlegel, H. B.; Scuseria, G. E.; Robb, M. A.; Cheeseman, J. R.; Scalmani, G.; Barone, V.; Mennucci, B.; Petersson, G. A.; Nakatsuji, H.; Caricato, M.; Li, X.; Hratchian, H. P.; Izmaylov, A. F.; Bloino, J.; Zheng, G.; Sonnenberg, J. L.; Hada, M.; Ehara, M.; Toyota, K.; Fukuda, R.; Hasegawa, J.; Ishida, M.; Nakajima, T.; Honda, Y.; Kitao, O.; Nakai, H.; Vreven, T.; Montgomery, J. A., Jr.; Peralta, J. E.; Ogliaro, F.; Bearpark, M.; Heyd, J. J.; Brothers, E.; Kudin, K. N.; Staroverov, V. N.; Kobayashi, R.; Normand, J.; Raghavachari, K.; Rendell, A.; Burant, J. C.; Iyengar, S. S.; Tomasi, J.; Cossi, M.; Rega, N.; Millam, J. M.; Klene, M.; Knox, J. E.; Cross, J. B.; Bakken, V.; Adamo, C.; Jaramillo, J.; Gomperts, R.; Stratmann, R. E.; Yazyev, O.; Austin, A. J.; Cammi, R.; Pomelli, C.; Ochterski, J. W.; Martin, R. L.; Morokuma, K.; Zakrzewski, V. G.; Voth, G. A.; Salvador, P.; Dannenberg, J. J.; Dapprich, S.; Daniels, A. D.; Farkas, Ö.; Foresman, J. B.; Ortiz, J. V.; Cioslowski, J.; Fox, D. J. *Gaussian 09*, Revision D.01; Gaussian, Inc.: Wallingford, CT, 2009.

(73) Schlegel, H. B. *J. Comput. Chem.* **1982**, *3*, 214.

(74) Peng, C.; Ayala, P. Y.; Schlegel, H. B.; Frisch, M. J. *J. Comput. Chem.* **1996**, *17*, 49.

(75) Gonzalez, C.; Schlegel, H. B. *J. Chem. Phys.* **1989**, *90*, 2154.

(76) Gonzalez, C.; Schlegel, H. B. *J. Phys. Chem.* **1990**, *94*, 5523.

(77) Lee, C. T.; Yang, W. T.; Parr, R. G. *Phys. Rev. B: Condens. Matter Mater. Phys.* **1988**, *37*, 785.

(78) Hehre, W. J.; Ditchfield, R.; Pople, J. A. *J. Chem. Phys.* **1972**, *56*, 2257.

(79) Clark, T.; Chandrasekhar, J.; Spitznagel, G. W.; Schleyer, P. V. R. *J. Comput. Chem.* **1983**, *4*, 294.

(80) Ricca, A.; Bauschlicher, C. W., Jr; Bakes, E. L. O. *Icarus* **2001**, *154*, 516.

(81) Ricca, A.; Bauschlicher, C. W.; Rosi, M. *Chem. Phys. Lett.* **2001**, *347*, 473.

(82) Coates, A. J.; Wellbrock, A.; Lewis, G. R.; Jones, G. H.; Young, D. T.; Crary, F. J.; Waite, J. H.; Johnson, R. E.; Hill, T. W.; Sittler, E. C. *Faraday Discuss.* **2010**, *147*, 293.

(83) Coates, A. J.; Crary, F. J.; Lewis, G. R.; Young, D. T.; Waite, J. H.; Sittler, E. C. *Geophys. Res. Lett.* **2007**, *34*, L22103.

(84) Wren, S. W.; Vogelhuber, K. M.; Garver, J. M.; Kato, S.; Sheps, L.; Bierbaum, V. M.; Lineberger, W. C. *J. Am. Chem. Soc.* **2012**, *134*, 6584.

(85) Ervin, K. M. *Int. J. Mass Spectrom.* **2015**, *378*, 48.

(86) Eichelberger, B. R.; Snow, T. P.; Bierbaum, V. M. *J. Am. Soc. Mass Spectrom.* **2003**, *14*, 501.

(87) Yang, Z.; Eichelberger, B.; Carpenter, M. Y.; Martinez, O., Jr.; Snow, T. P.; Bierbaum, V. M. *Astrophys. J.* **2010**, *723*, 1325.

(88) Faure, A.; Vuitton, V.; Thissen, R.; Wiesenfeld, L.; Dutuit, O. *Faraday Discuss.* **2010**, *147*, 337.